AN ENERGY HARVESTER FOR ROTATING ENVIRONMENTS USING OFFSET PENDULUM DYNAMICS

S. J. Roundy[1], and J. Tola*

[1]University of Utah, Department of Mechanical Engineering, Salt Lake City, UT, USA

ABSTRACT

We present an energy harvester for environments that rotate through the earth's gravitational field. Example applications include shafts connected to motors, axles, propellers, fans, and wheels or tires. Our approach makes use of the unique dynamics of an offset pendulum along with a nonlinear bi-stable restoring spring to improve the operational bandwidth of the system. We apply our approach to a tire pressure monitoring system (TPMS) that is mounted on a car rim. Simulation and experimental test results show that the prototype generator is capable of directly powering an RF transmission every 60 seconds or less over a speed range of 6 to 95 mph.

KEYWORDS

Energy harvesting, rotating environments, piezoelectrics, wideband power generation, TPMS

INTRODUCTION

The ability to harvest or scavenge energy from a wireless sensor's operating environment can enable many sensing applications in which regularly replacing or recharging batteries is either not possible or expensive [1][2]. Many potential sources of energy have been studied, including vibrations [3], temperature gradients [4], and human motion [5]. Harvesting energy from a rotating environment (i.e. rotating machinery, wheels, shafts, propellers, etc.) may be considered a subset of vibration energy harvesting, but has unique dynamics that benefit from different solutions. A tire pressure monitoring systems (TPMS) is a good example of an application in which energy harvesting from a rotating environment is beneficial. TPMS modules are mounted on the car rim, attached to inside of the valve stem. The system is subjected to a +/- 1G excitation at the rolling frequency as the wheel rotates through the earth's gravitational field. (See Figure 1).

Most vibration energy harvesting systems operate effectively only at resonance. Thus, for both linear and rotational systems, the narrow operating bandwidth is a chief limitation. The following three main approaches to improving the bandwidth are the subjects of current research efforts: tuning the resonance frequency of the harvester during operation [6][7], implementing multi-mode oscillators [8], and employing non-linear oscillators to widen the bandwidth [9]. These methods are equally applicable to rotational systems. Gu and Livermore [10] have used the dynamics of an offset pendulum in order to increase the harvester bandwidth for rotational systems.

In this study we present the analysis, implementation, and test results for an approach to harvesting energy from a rotating environment. While we specifically apply our design to the TPMS application, it is applicable to any rotating environment in which the axis of rotation is more or less parallel to the earth's surface (i.e. horizontal). Like Gu and Livermore [10], our approach takes advantage of the unique features of the dynamics of an offset pendulum to create an inherently broad frequency response. In addition, it contains many unique features that enable efficient power harvesting under the realistic constraints of a TPMS system, and many rotational systems in which the harvester must be small compared to the rotation radius. Finally, our system incorporates a nonlinear bi-stable oscillatory motion to further enhance the bandwidth.

The remainder of this paper is organized as follows. We first present modeling and analysis of the key dynamic effects that we are exploiting. We then discuss the details of the prototype design. And finally, we present and discuss the experimental results.
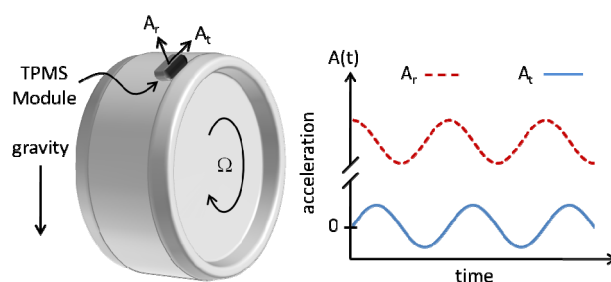

Figure 1. Illustration of TPMS module mounted to a rim. Directions of tangential (At) and radial (Ar) acceleration shown along with representative time traces for these two signals.

OFFSET PENDULUM DYNAMICS

Figure 2 shows an offset pendulum system mounted on a rotating cylinder or wheel. If the angle (θ) is small, the centripetal acceleration acts like a linear spring bringing the proof mass back to the center ($\theta = 0$). The effective resonance of this pendulum system is given by equation 1. If distance of the pendulum from the center of rotation (L_1) is equal to the length of the pendulum (L_2), the resonance will always equal the rotating frequency (Ω). A proof mass moving in a curved track whose radius of curvature is one half the primary rotation radius exhibits the same behavior as an offset pendulum. Note that this analysis assumes the proof mass is a point mass.

$$\omega_n = \Omega \sqrt{\frac{L_1}{L_2}} \qquad (1)$$

In our target application, the radius is large, and the system operates at relatively low frequencies. Thus the displacement of the proof mass, if unconstrained, will be

quite large. Equation 1 only applies under the small angle approximation. Furthermore, in a practical system, the proof mass displacement must be constrained. Figure 3 illustrates the limits of both the small angle approximation and practical displacement limits for a standard car rim and tire. If the displacement is large enough to reach the end stops (4mm in Figure 3), the system is no longer a freely oscillating resonant structure, so any resonance frequency error associated with the small angle approximation is not relevant. From Figure 3, the error at a displacement limit of +/- 4mm is less than 0.01%. In fact the displacements could be much larger before significant errors (> 1%) occur.
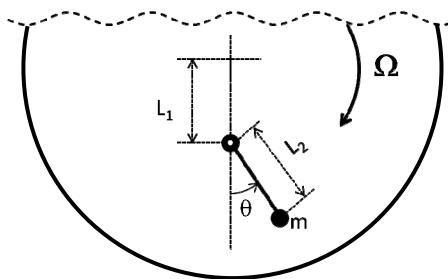

Figure 2: Illustration of an eccentrically mounted pendulum on rotating wheel or shaft. The centripetal acceleration on the proof mass acts like a linear spring as long as θ is small.
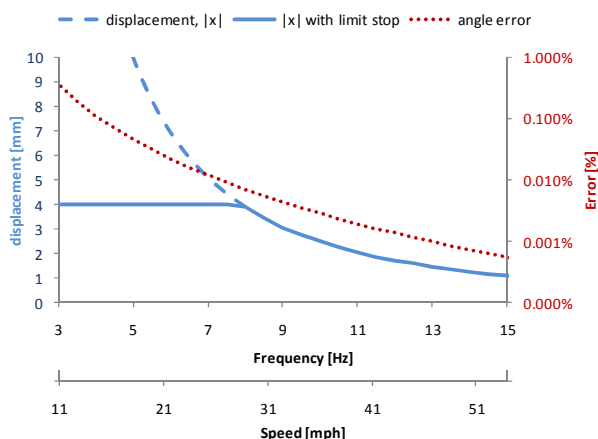

Figure 3. Proof mass displacement amplitude and error resulting from the small angle approximation vs. rolling frequency and speed. A rim diameter of 15 inches (38cm), and a tire rolling diameter of 20 inches (51 cm) was assumed. Limit stop is at a 4mm displacement.

PROTOTYPE DESIGN AND DISCUSSION

A few practical application related constraints drove many of the design implementation decisions. First, the system must generate enough power to support transmissions once per minute even at very slow speeds (~ 10 mph). This constraint necessitates relatively large allowable displacements (~ +/- 2.5 mm). Second, the height (i.e. size in the radial direction) must be small because of tire and rim geometry, which rules out a cantilever structure extending in the radial direction or an actual pendulum as shown in Figure 2.

An illustration of the solution employed is shown in Figure 4. We implemented a curved track with a radius smaller than the rim radius to implement the offset pendulum dynamics. The proof mass is a steel ball bearing that rolls back and forth along the curved track. This system can withstand the very large static centripetal load while still maintaining low friction motion in the tangential direction. In order to improve the harvesting of energy at low rotating frequencies, we employed spring loaded end stops.

The transducers are two piezoelectric beams running along the length of the track, one on each side. The beam and proof mass make contact through a smaller ball held in a conical hole along the side of the track. As the proof mass rolls past the smaller ball, the smaller ball gets pushed out and deflects the piezoelectric beam. This process is illustrated in Figure 5. For clarity, Figure 5 shows only one piezoelectric beam. There are two piezoelectric actuation cycles per tire revolution per beam.
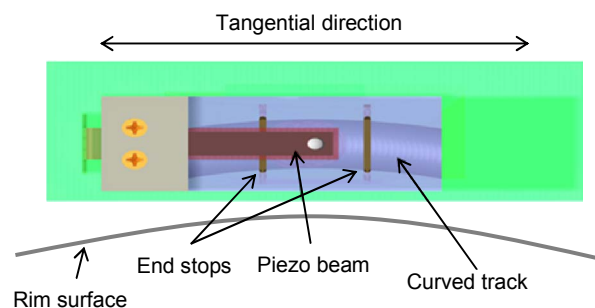

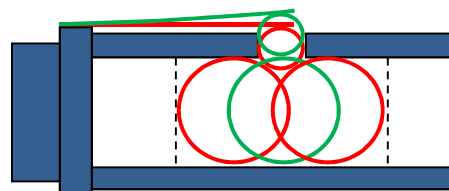
Figure 4: Illustration of energy harvester concept.

Figure 5: Illustration of piezoelectric beam actuation. When proof mass ball is in the position on the left or right (shown in red) the piezoelectric beam is undeflected. When the proof mass ball is in the center position (shown in green), the piezoelectric beam is deflected.

We decided to use piezoelectric rather than electromagnetic transduction because at low frequencies the voltage from the electromagnetic system would be very low and require more complex power electronics. As piezoelectric devices are generally stiff, they are best actuated in a high force, low displacement mode. The mechanical actuation system shown in Figure 5 is essentially a force amplification mechanism, so the lower force, higher displacement motion of the proof mass is converted to a higher force, lower displacement motion for the piezoelectric beam. A second benefit of the actuation system shown is that it is inherently immune to reliability concerns from over-travel.

The interaction of the proof mass with the piezoelectric beams as well as with the spring loaded end

stops alters the effective spring constant of the system. Figure 6 shows the effective spring force on the proof mass at very slow speeds (i.e. neglecting the effect of the centripetal acceleration). The location of the spring loaded end stops is clearly indicated. Throughout most of the proof mass motion, there is a negative spring constant, meaning that the spring force pushes the proof mass away from the zero displacement point. The gravitational force on the proof mass is also shown for the case where the tangential axis is aligned with gravity. This shows that the gravitational force is strong enough to push the proof mass through its entire range of motion at low speed. The system results in a double well potential function (see Figure 7) that is characteristic of bi-stable oscillators. As the speed increases, the effective stiffness from the centripetal acceleration increases, which changes the shape of the potential function. At high speeds, the potential function becomes more and more like that of a standard linear spring as the effect of the centripetal acceleration dominates over the restoring force from the proof mass interaction with the piezoelectric beam.
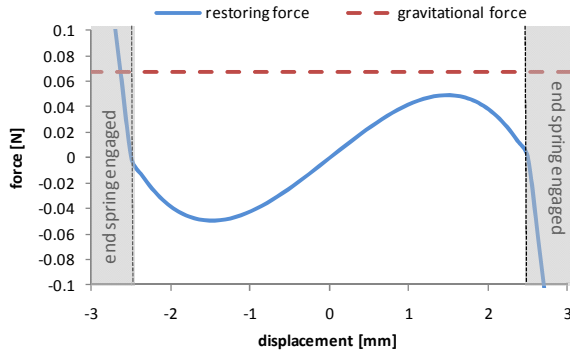

Figure 6. Effective spring (restoring) force and gravitational force on the proof mass over its range of motion. Gravitational force assumes the tangential axis is aligned to gravity.
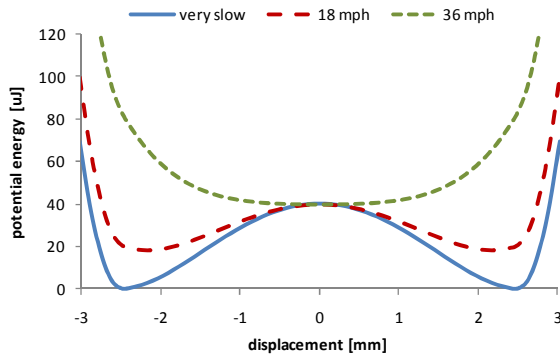

Figure 7: Shape of the nonlinear potential function. Three speeds shown: near 0 mph (very slow), 18mph, and 36 mph. At high speeds the potential function approaches that of a standard linear spring.

RESULTS

Given the extra forces from the interaction with the piezoelectric beam and the spring loaded end stops, the system is no longer always resonant as implied by Figure 2 and equation 1. However, the bandwidth of the device

is still significantly enhanced compared to a simple linear oscillator. Figure 8 shows the simulated rms voltage across a matched resistor and the power output vs. frequency. We use the convergence to an average power ($\hat{P}$), given by equation 2, as the appropriate metric for this nonlinear system. At each frequency, the system simulation is allowed to run for a sufficient number of forcing periods such that any transients die out, then equation 2 is applied over k periods to get an average power generation value.

$$\hat{P} = \frac{1}{kT} \int_0^{kT} \frac{V(t)^2}{R_L} \, dt \qquad (2)$$

where k is the number of forcing periods, $T = 2\pi/\Omega$ is the period of the forcing oscillation, $V(t)$ is the generated voltage, and R_L is the load resistance.

The simulated output shown in Figure 8 indicates that the proof mass motion, and thus power output, drop dramatically at about 100 mph. The simulation models both viscous and coulomb friction. At very high speeds the displacements naturally go down, and the coulomb friction goes up. At around 100 mph, the friction overwhelms the motion of the system.
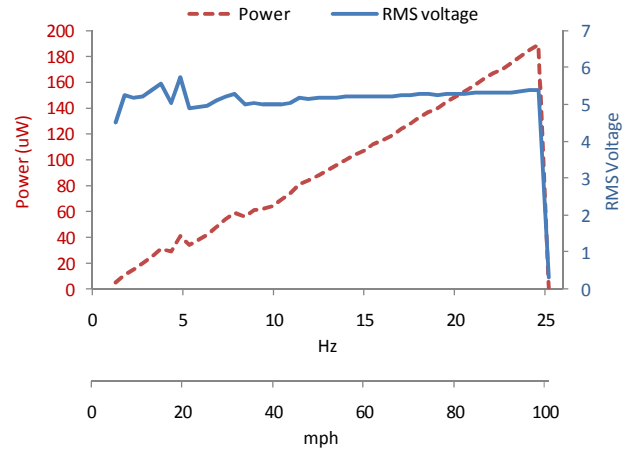

Figure 8: Simulated output voltage and power versus rotation frequency. Piezoelectric generator is terminated with a matched resistor.
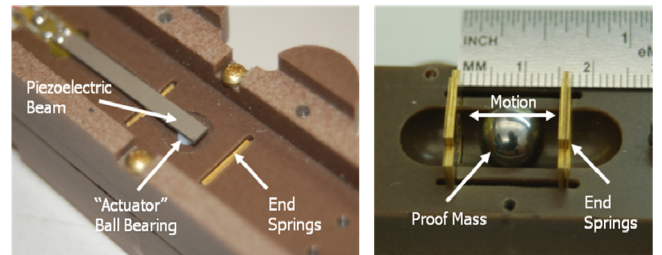

Figure 9. Prototype device used for road testing.

Several prototypes based on this concept were built and tested. One example is shown in Figure 9. The harvester output was measured via an optimally sized resistor terminating the piezoelectric beam. Figure 11 shows the voltage output across the load resistor

measured during road tests. The measured voltage is a little lower in magnitude and the pulse is narrower than the simulated voltage. These facts are probably indicative of an assembly tolerance issue such that there is a small gap between the piezoelectric beam and the actuator ball placed in the conical hole (see Figure 5) when the proof mass is at one end or the other.
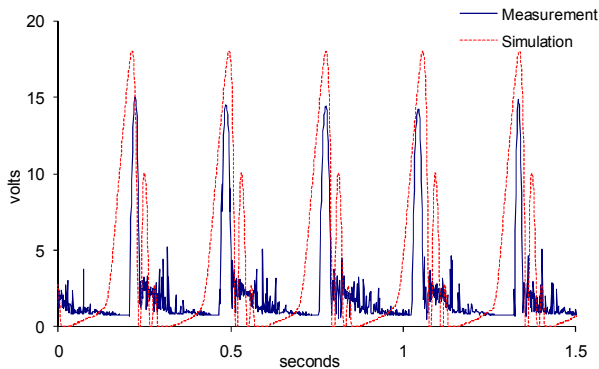

Figure 10. Simulated and measured open circuit voltage output. Tire is rolling at 10 mph.

The prototype was also used to power a wireless tire pressure monitoring system. Figure 11 shows the results of road tests performed with this system. The system performs well from speeds of 10 mph to 95 mph. The slow speed performance is particularly impressive and the system can support more than one transmission per minute down to speeds of 6 mph. At high speeds, above 95 mph, the increased rolling friction overcomes the inertial forces the time between transmissions climbs rapidly.
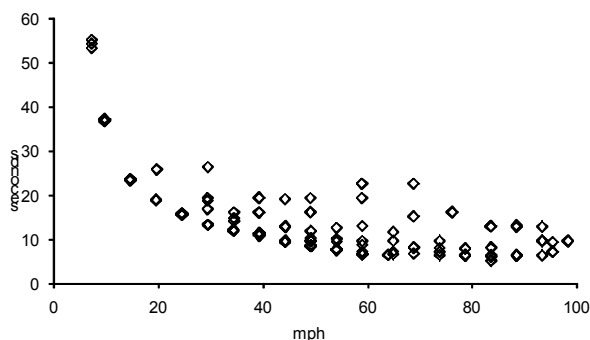

Figure 11: Experimental data showing the time between TPMS transmissions for a rim mounted energy harvester. Data shown for multiple tests on three different devices.

CONCLUSIONS

We have demonstrated an energy harvester for a rotating environment in which the axis of rotation is horizontal. The solution makes use of the dynamics of an offset pendulum to increase the operational bandwidth. The combination of restoring forces acting on the system, including centripetal acceleration and restoring forces of the piezoelectric beams, creates a nonlinear bi-stable oscillator. The frequency response of the system is significantly broader than a standard linear oscillator

system. The system was applied to a tire pressure monitoring system and was able to support better than one transmission per minute in the speed range of 6 to 95 mph, and more than 3 transmissions per minute from 20 to 95 mph.

REFERENCES

[1] P. D. Mitcheson, E. M. Yeatman, G. K. Rao, A. S. Holmes, and T. C. Green, "Energy Harvesting From Human and Machine Motion for Wireless Electronic Devices," *Proceedings of the IEEE*, vol. 96, no. 9, pp. 1457–1486, 2008.

[2] C. Knight, J. Davidson, and S. Behrens, "Energy Options for Wireless Sensor Nodes," *Sensors*, vol. 8, no. 12, pp. 8037–8066, Dec. 2008.

[3] S. Roundy, P. K. Wright, and J. Rabaey, "A study of low level vibrations as a power source for wireless sensor nodes," *Computer Communications*, vol. 26, no. 11, pp. 1131–1144, Jul. 2003.

[4] M. Strasser, R. Aigner, M. Franosch, and G. Wachutka, "Miniaturized thermoelectric generators based on poly-Si and poly-SiGe surface micromachining," *Sensors and Actuators A: Physical*, vol. 97–98, pp. 535–542, Apr. 2002.

[5] J. M. Donelan, Q. Li, V. Naing, J. a Hoffer, D. J. Weber, and a D. Kuo, "Biomechanical energy harvesting: generating electricity during walking with minimal user effort.," *Science*, vol. 319, no. 5864, pp. 807–10, Feb. 2008.

[6] V. R. Challa, M. G. Prasad, Y. Shi, and F. T. Fisher, "A vibration energy harvesting device with bidirectional resonance frequency tunability," *Smart Materials and Structures*, vol. 17, no. 1, p. 015035, Feb. 2008.

[7] C. Peters, D. Maurath, W. Schock, F. Mezger, and Y. Manoli, "A closed-loop wide-range tunable mechanical resonator for energy harvesting systems," *Journal of Micromechanics and Microengineering*, vol. 19, no. 9, p. 094004, Sep. 2009.

[8] Q. Ou, X. Chen, S. Gutschmidt, A. Wood, N. Leigh, and a. F. Arrieta, "An experimentally validated double-mass piezoelectric cantilever model for broadband vibration-based energy harvesting," *Journal of Intelligent Material Systems and Structures*, vol. 23, no. 2, pp. 117–126, Feb. 2012.

[9] S. C. Stanton, C. C. McGehee, and B. P. Mann, "Nonlinear dynamics for broadband energy harvesting: Investigation of a bistable piezoelectric inertial generator," *Physica D: Nonlinear Phenomena*, vol. 239, no. 10, pp. 640–653, May 2010.

[10] L. Gu and C. Livermore, "Compact passively self-tuning energy harvesting for rotating applications," *Smart Materials and Structures*, vol. 21, no. 1, p. 015002, Jan. 2012.